First-Principles Study of the Structures and Vibrational Frequencies for Tetrathiafulvalene TTF and TTF-d_4 in Different Oxidation States

C. Katan[†]

Groupe Matière Condensée et Matériaux, UMR-CNRS 6626, Université Rennes I, Campus de Beaulieu, F-35042 Rennes Cedex, France

Received: October 1, 1998

The structures and vibrational spectra of tetrathiafulvalene (TTF), TTF-d_4, and their radical cations have been extensively studied using the projector augmented wave method, which allows first-principles molecular dynamics based on the density functional theory. The dependence of the bond lengths and vibrational frequencies on the molecular ionicity is discussed, and the ionization energy, Coulomb repulsion, and spin-splitting parameter are also derived.

I. Introduction

Tetrathiafulvalene (TTF), shown in Figure 1, is a well-known electron donor molecule used in the synthesis of a great variety of charge transfer salts ranging from insulators to metals. Some of its derivatives, complexed to appropriate electron acceptors, form organic superconductors showing quasi one- or two-dimensional packings. In spite of its popularity, no thorough examination of its properties has ever been undertaken and most effort has been concentrated on its derivatives that lead to relatively high-temperature ambiant pressure organic superconductors, namely, bis(ethylenedithio)tetrathiafulvalene (BEDT-TTF).[1−3]

The structure of TTF has been often discussed in terms of D_{2h} symmetry, which assumes a planar structure for the whole molecule. Only recently has a gas phase electron diffraction study showed that a nonplanar boat structure gives the best fit to the observed intensity patterns.[4] This was corroborated by very recent density functional calculations that pointed out the small energy difference between planar and boatlike conformations.[1] For this reason, TTF is very flexible and can appear in various conformations depending on the donor−donor and donor−acceptor interactions in the crystal. Moreover, the corresponding boat-deformation vibrational mode has a very low frequency.[1] This mode may play a special role in some of the phase transitions occurring in the TTF-based charge transfer salts through its possible coupling with the charge transfer or some lattice mode. In the case of BEDT-TTF, it has been suggested that the coupling between the charge transfer and this mode could be responsible for the superconductivity.[2]

One of the characteristics of charge transfer crystals is the ionicity of the molecules, i.e., the value of the charge transfer from the donor molecule to the acceptor. Most commonly, the estimate of this charge transfer is based on the dependence of some bond lengths or some vibrational frequencies on the molecular ionicity. These relations are deduced from the experimental data obtained with a set of compounds expected to have known oxidation states, but they have seldom been verified theoretically. Such a verification is desirable for TTF, as it is a widely used electron donor.

[†] Fax: 33 2 99 28 67 17. E-mail: Claudine.Katan@univ-rennes1.fr.

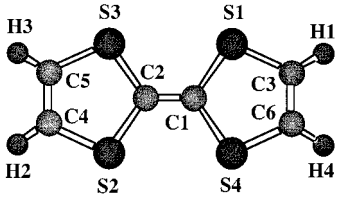

Figure 1. Definition of the atomic types for the atoms of the TTF molecule.

The aim of this paper is to provide a complete and consistent analysis of the static and dynamical properties of TTF-d_4 and TTF in different oxidation states with the projector augmented wave (PAW) method.[5] This method combines the first-principles molecular dynamics (MD) method of Car and Parrinello[6] with an all-electron electronic structure method that can be efficiently applied to all elements of the periodic table within the local density approximation (LDA) of density functional theory. Vibrational analysis is performed by fitting a system of harmonic oscillators to the MD trajectories.[7]

This paper is organized as follows: in section II we summarize all computational details. Section III is devoted to the structural properties of TTF in different oxidation states. In section IV we derive some model parameters: ionization energy, Coulomb repulsion, and spin-splitting parameter. Section V contains the analysis of the vibrational properties of TTF, TTF-d_4, and their radical cations.

II. Computational Details

All electronic structure and atomic trajectories calculations have been performed with the projector augmented wave (PAW) method.[5] This method combines the original fictitious Lagrangian approach of Car and Parrinello,[6] in which the atomic coordinates and the electronic wave function are treated simultaneously by a set of Newton's equations, with an efficient all-electron electronic structure scheme. It allows high-quality, energy-conserving, first-principles MD simulations even for large systems. The pseudopotential, partial waves, and projector functions have been constructed with the procedure described

10.1021/jp983941v CCC: $18.00
Published on Web 02/18/1999

TABLE 1: Calculated Bond Lengths (Å) and Angles (deg) for the TTF Molecule in Comparison with Gas Phase Electron Diffraction Results[a]

	PAW-LDA			PAW-BP			exp	calc
	TTF	$TTF^{+0.5}$	TTF^{+1} [b]	TTF	$TTF^{+0.5}$	TTF^{+1}	(ref 4)	(ref 1)
C−H	1.095(5)	1.095	1.096	1.092(2)	1.092	1.092	1.105	1.084
C_1-C_2	1.354(3)	1.372	1.393	1.361(59)	1.378	1.398	1.358	1.350
C_1-S_1	1.733(7)	1.720	1.706	1.777(8)	1.761	1.745	1.767	1.788
C_3-S_1	1.721(17)	1.708	1.698	1.764(62)	1.753	1.743	1.753	1.764
C_3-C_6	1.339(9)	1.343	1.348	1.351(0)	1.354	1.359	1.348	1.337
$C_2C_1S_1$	122.7(6)	122.5	122.5	122.4(1)	122.1	122.1	122.9	123.2
$S_1C_1S_4$	114.5(8)	114.9	114.9	115.2(9)	115.9	115.9	114.2	113.7
$H_1C_3S_1$	117.9(8)	118.0	118.1	117.5(5)	117.6	117.7	117.8	117.1
$C_1S_1C_3$	94.4(5.1)	95.4	95.8	93.6(9)	94.3	94.7	94.5	94.7
$C_6C_3S_1$	117.2(5)	117.1	116.8	117.9(8.2)	117.8	117.3	117.6	118.0 0
θ	17(0)	0	0	15(0)	0	0	13.5	9.9

[a] θ corresponds to the dihedral angle between $S_1C_1S_4$ and $S_1C_3C_6S_4$ planes. [b] Spin-polarized calculations lead to the same values.

in ref 5 for nontransition metals. One projector function per angular-momentum quantum number was used for s- and p-angular momenta. The pseudowave functions were expanded into plane waves up to a kinetic energy cutoff of 30 Ry. Most of the calculations were non-spin-polarized and within the LDA (denoted PAW-LDA), using the LDA parametrization by Perdew and Zunger[8] based on Monte-Carlo simulations of the free electron gas by Ceperley and Adler.[9] Nevertheless, a few spin-polarized calculations were done to calculate the spin-splitting parameter and to check the validity of the non-spin-polarized calculations. We also performed calculations that included Becke's gradient correction to the exchange energy[10] and Perdew's gradient correction for the correlation energy[11] (denoted PAW-BP or BP). The calculations were carried out using a face-centered cubic supercell with a side length of $a =$ 40 au. In all calculations the molecule had been electrostatically decoupled from its periodic images as described in ref 12, and by changing the lattice vectors, we verified that this supercell was sufficiently large to allow a good description of an isolated molecule.

The initial geometry for the MD simulations was obtained from the optimized geometry of the molecule in its ground state by adding a random distribution of atomic velocities corresponding to 30 K. During the MD simulation, an average temperature of 30 K was maintained using a Nosé thermostat[13] with an eigenfrequency of 5 THz. The Verlet algorithm[14] was used with a time step of 8 au for a total simulation time of about 3 ps. To prevent deviations from the Born−Oppenheimer surface, a small constant friction was also applied to the dynamics of the electronic wave functions.

The atomic trajectories obtained by MD simulations are analyzed in terms of harmonic vibrations using the technique developed by Margl and co-workers.[7] This approach, which is similar to Kohanoff's[15] except for the penalty function used for the least-squares fit, fits the trajectories of a harmonic system to those obtained from the MD simulation. The fit parameters are the eigenvectors of the dynamical matrix, the amplitudes, and the frequencies. The MD simulations were carried out for the deuterated molecule, and by renormalizing the dynamical matrix according to the atomic masses,[7] the eigenfrequencies and eigenmodes for the hydrogenated molecule were determined using the molecular point group of the ground state of the considered molecule. After the angular momentum of the entire molecule was removed, each complete trajectory was split into mutually orthogonal partial trajectories belonging to the different irreducible representations. For each subtrajectory, the fitting procedure was used to determine the eigenmodes and eigenfrequencies of that symmetry. The accuracy of the vibrational modes was checked by examining the vibrational spectrum obtained when the subtrajectory was projected onto a specified eigenvector. For a satisfactory set of eigenvectors, each projection yielded a single, well-defined peak. Moreover, we verified that the residual trajectory remaining after all modes had been removed was composed only of noise.

III. Structural Properties

In this section we will focus on the structural properties of an isolated TTF molecule in different oxidation states. According to the gas phase electron diffraction results and to the recent density functional B3LYP[16] and ab-initio MP2 calculations of Liu and co-workers,[1] we found that neutral TTF has a boatlike C_{2v} symmetry equilibrium structure. The corresponding bond lengths and angles are given in Table 1. The dihedral angle between $S_1C_1S_4$ and $S_1C_3C_6S_4$ planes is somewhat overestimated in pure LDA calculations and improved by using BP gradient corrections. For all other angles, LDA gives the best results in comparison to experiment. This is no more true for the bond lengths for which LDA gives a systematic underestimate whereas BP somewhat overestimates them except the C−H one. From these values it is clear that the global agreement with the electron diffraction results is better with LDA or BP gradient corrections than with the B3LYP method.

When optimizing TTF's geometry, one reaches very easily the planar conformation instead of the true boatlike C_{2v} ground state. In particular, when the initial configuration has a D_{2h} symmetry, the initial symmetry remains unaltered by atomic relaxation.[17] The numbers listed in brackets in Table 1 show that except for θ, bond lengths and angles are little affected by the boat deformation. The energy difference between the planar and boat structures is 0.02 eV within LDA and 0.04 eV with BP gradient corrections. In our simulations no stable chairlike conformation has been obtained but, interestingly, the energy difference between planar and chair structure (with the same bond length and angles as for the boat structure) is only of 0.02 eV. These small energy differences show that the TTF molecule is highly flexible and intermolecular interactions may lead to preferences for either conformation.[18−20]

Of course, the molecular structure in a crystal will also be affected by the rate of electron transfer between donor and acceptor. This fact has been widely used as a tool to estimate the ionicity of molecules in charge transfer salts.[20,21−23] The correlation between charge and geometry is based on a linear variation of either a single bond length[20] or a function (ratio, difference, ...) of several bond lengths.[21−23] In order to verify these relations we have optimized the geometry of four oxidation states of the TTF molecule. The corresponding bond lengths

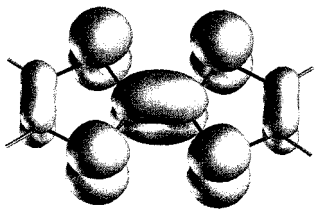

Figure 2. Isodensity representation of the HOMO of the TTF molecule.

and angles for $TTF^{+0.5}$ and TTF^{+} are given in Table 1. As soon as the molecule bears a positive charge, the planar D_{2h} structure becomes more stable. The same behavior has been reported for BEDT-TTF^{+}.[2] Our calculations show that all bond lengths change essentially linearly with the charge, the central C═C bond being the most strongly affected. The highest occupied molecular orbital (HOMO) of the TTF molecule,[24,25] shown in Figure 2, is π-antibonding with respect to the C—S bonds and π-bonding with respect to the C═C bonds, thus the C—S distances decrease while the C═C increase. As for the neutral molecule, the bond lengths are somewhat underestimated within LDA and overestimated with BP gradient corrections. Nevertheless, the obtained bond length variations are all consistent with the experimental data used to determine the relation between bond length and molecular ionicity.

However, one should keep in mind that these linear relations between bond length and molecular ionicity become approximate as soon as the molecule is no more isolated. Short intermolecular interaction such as S···S or C···S[26] often modify strongly the molecular geometry. In TTF-CA for example, the four S_1—C_1 bonds of one single TTF molecule become inequivalent at low temperature and their bond lengths range from 1.719 to 1.750 Å.[19] In a simple linear scheme, the lowest bond length would correspond to a charge of one electron whereas the highest would practically correspond to a neutral molecule. Sometimes the relation fails completely when the observed bond length is out of range, as for example, for the central C═C bond length (1.319 Å) in TTF-IA.[27]

IV. Model Parameters

The large unit cells characterizing the molecular charge transfer crystals often prevent the study of their physical properties by first principles calculations. The understanding of their behavior, particularly their phase transitions, is usually based on model calculations where the solid is described in terms of the frontier orbitals of the molecular moieties. These models are often derived from the Hubbard model and contain part or all of the following parameters: site energy difference between donor and acceptor, transfer integrals, on site Coulomb repulsion, intersite Coulomb interaction, electron-lattice phonon and electron-molecular vibration couplings, ... Depending on the relative values of these parameters, one can obtain qualitatively different results, which makes their choice crucial. Nowadays, a reliable estimate of them can be deduced from ab-initio calculations for isolated molecules,[17,28] dimers,[29] clusters, or crystals.[26]

Here we determine the relevant model parameters for electron transfer processes from a TTF molecule in charge transfer complexes. The HOMO of TTF is the relevant orbital involved in such processes. The results of our first principles calculations for a planar monomer in different oxidation states are given in Table 2. In order to deduce the Coulomb repulsion and the spin-splitting parameters, we combine our calculations with the simple model energy function proposed by Carloni and co-workers.[30] In this model the energy of an isolated species is given by

TABLE 2: PAW-LDA Calculated Total Energy and Energy of the HOMO State for Different Total or Spin-Up and Spin-Down Occupations of the HOMO State(s)[a]

occupations ($n_\uparrow$, $n_\downarrow$)	ϵ_{HOMO}	E_{Tot}	U	J
$n_\uparrow = n_\downarrow = 1.0$	−3.960	−2127.1494		
$n_\uparrow = n_\downarrow = 0.75$	−6.188	−2124.6141	4.44	
$n_\uparrow = n_\downarrow = 0.5$	−8.451	−2120.9555	4.47	
$n_\uparrow = 1.0$	−8.575	−2121.0178		0.12
$n_\downarrow = 0.0$	−8.323			

[a] Deduced values for the Coulomb repulsion U and the spin-splitting parameter J. All energies are given in eV.

$$E[\Delta n_\uparrow, \Delta n_\downarrow] = \bar{E} + \bar{\epsilon}(\Delta n_\uparrow + \Delta n_\downarrow) + \frac{1}{2}U(\Delta n_\uparrow + \Delta n_\downarrow)^2 - \frac{1}{2}J(\Delta n_\uparrow - \Delta n_\downarrow)^2 \quad (1)$$

where $\bar{E}$ is the total energy of the reference state, $\bar{\epsilon}$ is the energy of the relevant orbital in the reference state, U is the Coulomb repulsion of an electron in that orbital, J is the spin-splitting parameter or exchange coupling, and ($\Delta n_\uparrow$, $\Delta n_\downarrow$) is its occupation relative to the reference state.

The estimates of U for each occupation when taking the double occupied HOMO state as reference are given in Table 2. The same result of about 4.5 eV is obtained when taking the singly occupied HOMO state as reference. When BP gradient corrections are used, this value remains almost unchanged. It compares well to the previously theoretically inferred values for TTF[31] and some of its derivatives.[29,31] It is also very close to the one obtained for the electron acceptor CA,[28] with which TTF combines to form a mixed stack charge transfer salt.[19]

From the expansion of $E[\Delta n_\uparrow, \Delta n_\downarrow]$, one can estimate the spin-splitting parameter J independently from the estimate of the Coulomb repulsion U. As reference state we take the equal occupations of half an electron for each spin state in the HOMO and compare it to the spin-polarized calculations for TTF^{+}. This yields a value of 0.12 eV for J, which is again comparable to that of CA.[28] The same value can also be deduced from the difference between the spin-up and spin-down energy levels of the spin-polarized calculation.

An estimate of the ionization energy of TTF can be obtained either from the difference in total energy for the neutral molecule and the radical cation or from the mean value of the HOMO energy for TTF and TTF^{+}. Both ways yield 6.2 eV for pure LDA calculations and 6.3 eV with BP gradient corrections. These values compare well with those obtained by photoelectron spectroscopy in the gas phase (6.4 eV,[32] 6.7 eV[24]) and by quantum chemical calculations (6.8 eV[33]).

V. Vibrations

A good knowledge of the vibrational spectra of the electron donors such as TTF is very informative. In fact, intramolecular vibrations are commonly used to estimate the degree of ionicity of charge transfer crystals. Some of the vibrational frequencies strongly depend upon the electronic charge residing on them. A successful exploitation of the vibrational spectroscopy thus requires a clear identification of the frequency shifts upon ionization; that is, the changes of the vibrational frequencies in going from the neutral molecule to the fully charged molecular ion. Moreover, some of the physical properties of charge transfer

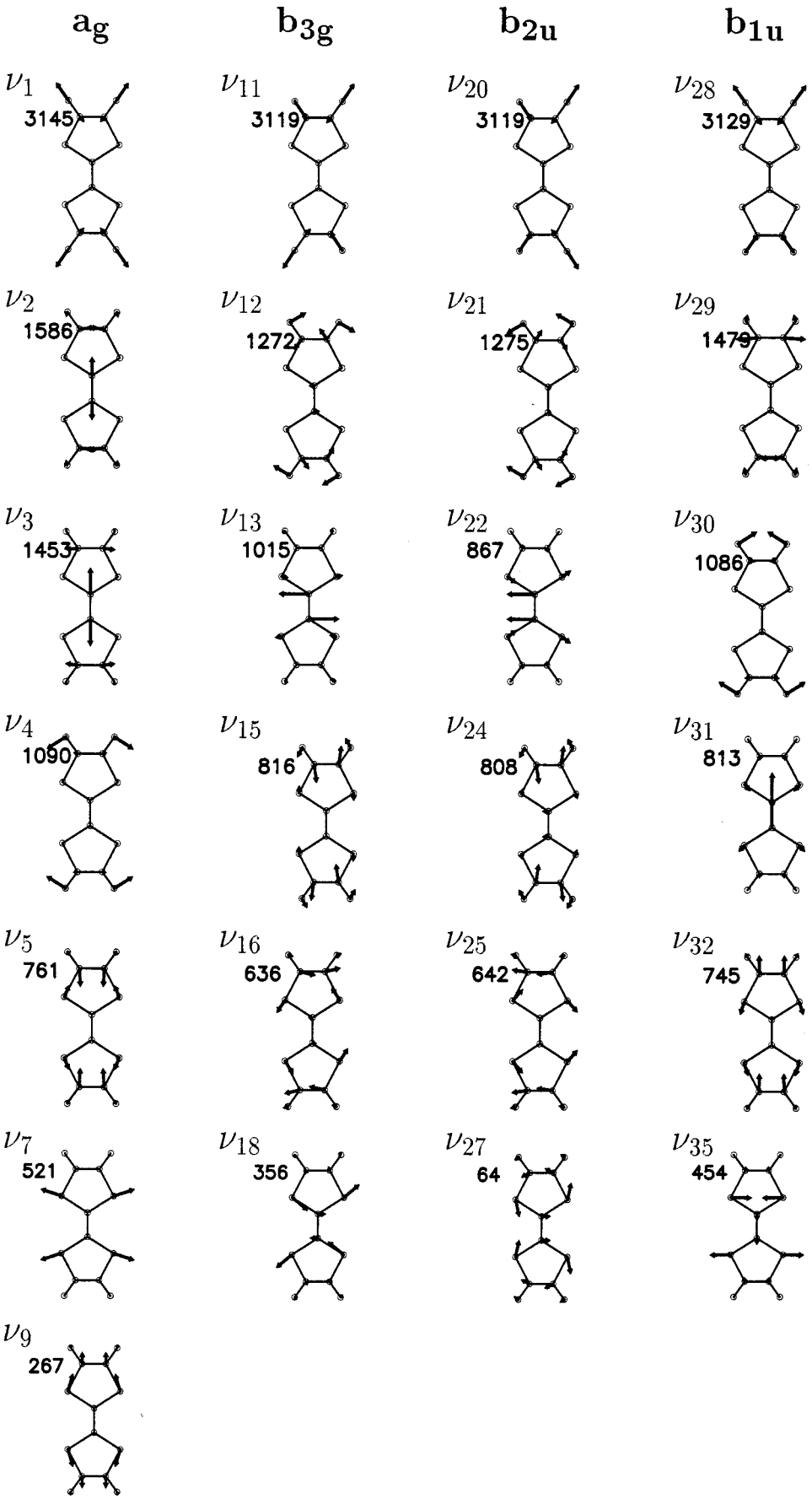

Figure 3. Calculated in-plane eigenvectors of $TTF^{+0.5}$. The numbers refer to the corresponding PAW-BP frequencies in cm^{-1}.

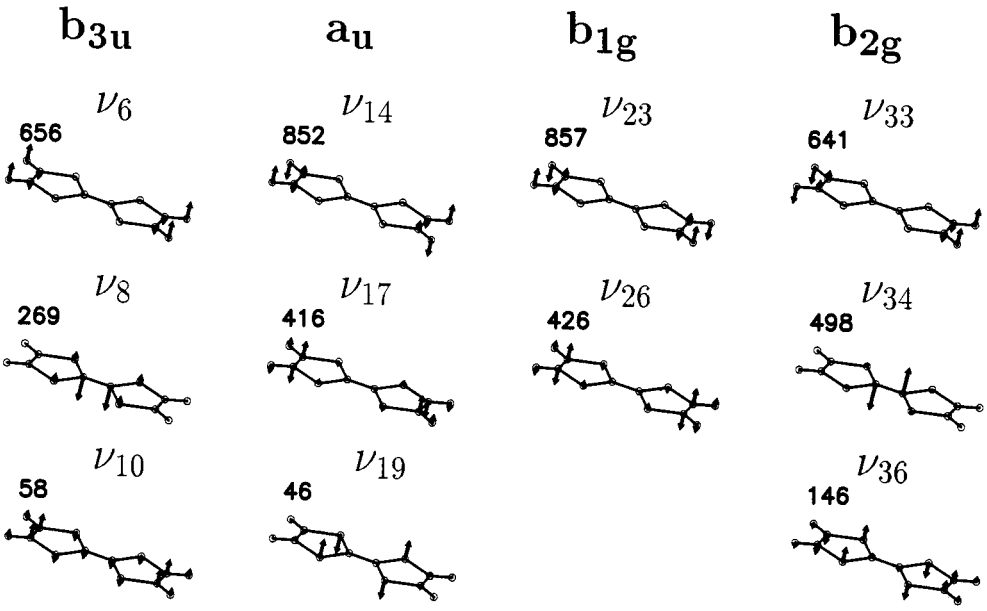

Figure 4. Calculated out-of-plane eigenvectors of $TTF^{+0.5}$. The numbers refer to the corresponding PAW-BP frequencies in cm^{-1}.

TABLE 3: Calculated Frequencies (cm^{-1}) for Various Charge States of the TTF Molecule Compared to Experimental Results of TTF in Solution and $(TTF)Br_{1.0}$ Crystalline Powders[35] and to Scaled B3LYP Values Calculated for an Isolated TTF[1,a]

			PANW-BP			exp[35]		calc[1]	PAW-BP	exp[35]
C_{2v}	D_{2h}		TTF	$TTF^{+0.5}$	TTF^{+1}	TTF	TTF^{+1}	TTF	$\Delta\nu$	$\Delta\nu$
a_1	a_g	ν_1	3124	3144	3155	3083	3075[a]	3095	+31	−1[b]
	a_g	ν_2	1570	1586[c]	1492	1555	1505	1569	−78	−50
	a_g	ν_3	1523	1453[c]	1390	1518	1420	1524	−133	−98
	a_g	ν_4	1088	1090	1086	1094	1078	1085	−2	−16
	a_g	ν_5	755	761	763	735	758	750	+8	+23
	b_{3u}	ν_6	630	656	680	639	705	640	+50	+65
	a_g	ν_7	521	511	474	501	478	−1	+27	
	b_{3u}	ν_8	284[c]	269	311	247[d]		264	+27	
	a_g	ν_9	225[c]	267	278	244	265	237	+53	+21
	b_{3u}	ν_{10}	55	58	76	(110)		30	+21	
a_2	b_{3g}	ν_{11}	3130	3119	3148	3072	3074[b]	3076	+18	0[b]
	b_{3g}	ν_{12}	1237	1272	1266	1258	1244[b]	1249	+29	−10[b]
	b_{3g}	ν_{13}	986	1015	1025	994	1066[b]	987	+39	+79[b]
	a_u	ν_{14}	843	852	866			859	+23	
	b_{3g}	ν_{15}	811	816	832	800	847[b]	813	+21	+23[b]
	b_{3g}	ν_{16}	632	636	635	612	661[b]	620	+3	+23[b]
	a_u	ν_{17}	422	416	422			402		
	b_{3g}	ν_{18}	354	356	350	308	322[b]	310		+13[b]
	a_u	ν_{19}	51	46	35			80	−16	
b_1	b_{2u}	ν_{20}	3111	3119	3144	3073	3063	3076	+33	−10
	b_{2u}	ν_{21}	1243	1275	1279	1254	1237	1246	+36	−17
	b_{2u}	ν_{22}		867	888	863	935[b]	860		+56[b]
	b_{1g}	ν_{23}	834	857	868			853	+34	
	b_{2u}	ν_{24}	791	808	826	794	825	808	+35	+31
	b_{2u}	ν_{25}		642	629	639	665[b]	630		+23[b]
	b_{1g}	ν_{26}	423	426	432	414[e]		404	+9	
	b_{2u}	ν_{27}		64	88	110	106[b]	111		+5[b]
b_2	b_{1u}	ν_{28}	3128	3129	3131	3108	3079	3095	+3	−29
	b_{1u}	ν_{29}	1533	1479	1419	1530	1478	1542	−114	−52
	b_{1u}	ν_{30}	1080	1085	1083	1090	1072	1084		−18
	b_{1u}	ν_{31}	798	813	834	781	836	785	+36	+55
	b_{1u}	ν_{32}	755	745	755	734	751	747		+17
	b_{2g}	ν_{33}	619	641	673			640	+54	
	b_{2g}	ν_{34}	497	498	510			507	+13	
	b_{1u}	ν_{35}	450	454	454	427	460	434	+4	+33
	b_{2g}	ν_{36}	105	146	176			79	+71	

[a] The last two columns give the calculated and experimental frequency shift between the neutral molecule and the radical cation. [b] Calculated from ref 35 [c] Mode mixing. [d] From monoclinic crystals. [e] From ref 40.

salts like conductivities or phase transitions are proposed to be related to electron-molecular vibrational couplings,[2,3,34] and a test of the role of this coupling can be achieved by isotope substitutions.[2]

Here we determine all 36 modes and eigenfrequencies of different oxidation states (0, +0.5, and +1) of TTF and TTF-d_4 using the technique briefly described in section II. For each case we have performed an MD simulation within the LDA

TABLE 4: Calculated Frequencies (cm^{-1}) for Various Charge States of the TTF-d_4 Molecule Compared to Experimental Results of TTF-d_4 in Solution and (TTF-d_4)$Br_{1.0}$ Crystalline Powders[35] and to Scaled B3LYP Values Calculated for an Isolated TTF-d_4[1,a]

			PAW-BP		exp[35]		calc[1]	PAW-BP		exp[35]	
C_{2v}	D_{2h}		TTF-d_4	TTF-d_4^{+1}	TTF-d_4	TTF-d_4^{+1}	TTF-d_4	$\Delta\nu$	$\Delta_{isotope}$	$\Delta\nu$	$\Delta_{isotope}$
a_1	a_g	ν_1	2330	2343	2280	2283[b]	2309	+13	794	−5[a]	803
	a_g	ν_2	1550	1460[c]	1544	1482	1555	−90	20	−62	11
	a_g	ν_3	1500	1383[c]	1504	1420	1502	−117	23	−84	14
	a_g	ν_4	776	782	787	755	778	+6	312	−12	307
	a_g	ν_5	739	746	715	741	733	+7	16	+26	20
	b_{3u}	ν_6	476	520	492	538	492	+44	154	+46	147
	a_g	ν_7	512	507	470	499	474	−5	0	+29	4
	b_{3u}	ν_8	281[c]	310	246[d]		263	+29	3		1
	a_g	ν_9	224[c]	275	242	265	235	+51	1	+23	2
	b_{3u}	ν_{10}	53	71	(108)		28	+18	2		
a_2	b_{3g}	ν_{11}	2297	2317	(2280)	2278[b]	2270	+20	833	+2[b]	796
	b_{3g}	ν_{12}	1061	1085	1057	1067[b]	1058	+24	176	+19[b]	201
	b_{3g}	ν_{13}	962	1000	975	1053[b]	968	+38	24	+68[b]	19
	a_u	ν_{14}	666	693			674	+27	177		
	b_{3g}	ν_{15}	711	730	(715)	752[b]	714	+19	100	+14[b]	85
	b_{3g}	ν_{16}	612	617	594	619[b]	604	+51	20	+17[b]	18
	a_u	ν_{17}	383	379			367	−4	39		
	b_{3g}	ν_{18}	351	345	305	319[b]	306	−6	3	+14[b]	3
	a_u	ν_{19}	50	35			80	−15	1		
b_1	b_{2u}	ν_{20}	2297	2312	2285	2275	2271	+15	814	−10	802
	b_{2u}	ν_{21}	1045	1057	1040	1041	1037	+12	198	+1	214
	b_{2u}	ν_{22}		887	865	919[b]	853		1	+64[b]	
	b_{1g}	ν_{23}	665	696			674	+31	169		
	b_{2u}	ν_{24}	706	724	703	731	708	+18	85	+28	91
	b_{2u}	ν_{25}		616	603	614	612		13	+11	36
	b_{1g}	ν_{26}	380	386	382[e]		369	+6	43		32
	b_{2u}	ν_{27}		111	108	103[b]	108		3	+5[b]	2
b_2	b_{1u}	ν_{28}	2327	2311	2337	2316	2309	−16	801	−21	771
	b_{1u}	ν_{29}	1501	1388	1508	1438	1507	−113	32	−70	22
	b_{1u}	ν_{30}	771	777	758	770	776	+6	309	+12	332
	b_{1u}	ν_{31}	797	833	779	828	785	+36	1	+49	2
	b_{1u}	ν_{32}	738	741	719	(731)	731	+3	17	+15[b]	15
	b_{2g}	ν_{33}	473	501			482	+28	146		
	b_{2g}	ν_{34}	503	527			515	+24			
	b_{1u}	ν_{35}	449	452	425	458	432	+3	1	+33	2
	b_{2g}	ν_{36}	100	168			76	+68	5		

[a] The last four columns give the frequency shift between the neutral molecule and the radical cation and the isotope shift. [b] Calculated from ref 35. [c] Mode mixing. [d] From monoclinic crystals. [e] From ref 40.

and another including BP gradient corrections. The symmetry of the vibrational modes was treated in the context of the C_{2v} molecular point group for the neutral species and the D_{2h} molecular point group for the charged ones. The 36 fundamental vibrations are classified into

$$C_{2v}: 10a_1 + 9a_2 + 8b_1 + 9b_2$$

$$D_{2h}: (7a_g + 3b_{3u}) + (6b_{3g} + 3a_u) + (6b_{2u} + 2b_{1g}) + (6b_{1u} + 3b_{2g})$$

using the designation commonly found in the litterature.[1,35] The vibrations belonging to a_g, b_{3g}, b_{2u}, and b_{1u}, representations are in-plane modes, whereas those belonging to b_{3u}, a_u, b_{1g}, and b_{2g} are out-of-plane.

The calculated eigenvectors of TTF are plotted in Figures 3 (in-plane) and 4 (out-of-plane). They provide a clear picture of all fundamental vibrations. They are consistent with the mode description given by Liu and co-workers[1] except for ν_{22} and ν_{23}. ν_{22} (b_{2u}) is predominantly a C−S stretching whereas ν_{23} (b_{1g}) corresponds to a C−H bending.

The corresponding frequencies, calculated with BP gradient corrections, are given in Table 3 together with the experimental results of TTF in solution and (TTF)$Br_{1.0}$ crystalline powders[35] and to scaled B3LYP values.[1] It is important to notice that, unlike Liu and co-workers,[1] we do not apply any scaling to our calculated values. In spite of the absence of scaling, our frequencies compare well with the available experimental and calculated values and provide a good reference for a number of experimentally unknown levels. On average, BP gradient corrections lead to better results than pure LDA (not reported here), which globally underestimates the frequencies. Within LDA, the C−H and C═C modes are largely underestimated whereas all modes having a large weight on the sulfur atoms (like C−S stretching) are more accurate than with BP. In both cases, the deviation for the low-frequency modes around 100 cm^{-1} and less is expected to be large. Owing to the finite simulation time, only a few periods of these modes are reproduced so that the estimate of their frequencies is less accurate.

Nevertheless, according to Liu and co-workers,[1] the experimental assignment of ν_{10} to 110 cm^{-1} is much higher than our calculated results, thus suggesting a misassignment. As can be seen in Figure 4, ν_{10} corresponds to the boat-deformation vibrational mode. Its unusual low frequency is favorable for its coupling to lattice modes and thus for its possible involvement in phase transitions occurring in TTF-based compounds. A recent low-frequency infrared study of TTF-CA[36] emphasized the critical behavior of two modes located around 30 cm^{-1} near the neutral-to-ionic phase transition. One of them has been assigned to the B_u *dimerization* lattice mode. The second one may correspond to the boat-deformation mode (b_{3u}) which could

couple to the dimerization mode and thus play an important role in this phase transition. Moreover, the observation of two coupled modes around 100 cm^{-1} in the Raman spectra of the ionic phase of TTF-CA[36,37] is consistent with our tentative interpretation as the frequency of ν_{10} increases with the molecular ionicity of TTF.

The frequency shifts between ionic and neutral molecules are in relatively good agreement with the experimental values. As found experimentally, there is no unique direction of shift for all fundamentals and its magnitude varies from 0 to about 100 cm^{-1}. Due to their large ionization shift, ν_{29} and ν_{31} are often used to estimate the charge residing on TTF.[38,39] Our calculated values show that these frequency shifts change indeed linearly, even if our absolute shifts do not completely agree with the experimental ones (LDA values are consistent with the reported BP values). But, unlike bond lengths, all frequencies do not change linearly because of mode mixing, especially between ν_2 and ν_3, which exchange their character. ν_8 and ν_9 are also strongly coupled when the molecule has a C_{2v} symmetry equilibrium structure. In any case, when using such a correlation between molecular ionicity and frequency shifts, one should always keep in mind the possible electron-intramolecular-vibration interaction[34] and the crystal field effect.

The calculated frequencies for different charge states and isotope shifts of TTF-d_4 are given in Table 4. They are in overall good agreement with the observed values.[35] Liu and co-workers[1] reported a significant difference between experiment and theory for ν_3, ν_9, ν_{25}, ν_{29}, and ν_{30}. We observe the same differences except for ν_9, for which there is a misprint in their paper for the observed frequency of TTF-d_4. All other experimentally unknown frequencies and isotope shifts are in very good agreement with those of Liu and co-workers, and they provide a guide for future searches. In Table 4 we have also reported the frequencies of TTF-d_4^+ and the corresponding frequency shifts, which again compare well to the experimental values.

VI. Conclusion

Using first principles calculations, we have thoroughly described the ground states and vibrations of TTF and TTF-d_4. We have confirmed that neutral TTF has a boatlike C_{2v} symmetry equilibrium structure whereas TTF^+ has a planar D_{2h} symmetry. The small energy differences between the different conformations of this molecule make it rather flexible. Due to its very low frequency, the boat-deformation mode of TTF can couple to lattice modes and we suggest that it may play an important role in the neutral-to-ionic phase transition of TTF-based mixed stack charge transfer compounds as well as in other phase transitions. By considering different oxidation states, we have demonstrated that the bond lengths and most of the vibrational frequencies of TTF and TTF-d_4 change linearly with molecular ionicity. This provides the first theoretical confirmation of this linearity, which is a fundamental assumption for the experimental determination of molecular ionicity. An estimate for the Coulomb repulsion, the spin-splitting parameter and the ionization energy have also been deduced. Whenever possible, comparison with experiment was made and an overall good agreement was found.

Acknowledgment. This work benefited from collaborations within and has been partially funded by the Human Capital and Mobility Network on "Ab initio (from electronic structure) calculation of complex processes in materials" (Contract No. ERBCHRXTC930369). Parts of the calculations have been supported by the "Centre National Universitaire Sud de Calcul" (France). I would like to thank P. Margl for his help concerning his VIB program and P. E. Blöchl for his PAW code and many useful discussions.

References and Notes

(1) Liu, R.; Zhou, X.; Kasmai, H. *Spectrochim. Acta A* **1997**, *53*, 1241.

(2) Demiralp, E.; Dasgupta, S.; Goddard, W. A., II. *J. Am. Chem. Soc.* **1995**, *117*, 8154.

(3) Williams, J. M.; Ferraro, J. F.; Thorn, R. J.; Carlson, K. D.; Geiser, U.; Wang, H. H.; Kini, A. M.; Whangbo, M.-H. *Organic Superconductors*; Prentice Hall: New Jersey, 1992.

(4) Hargittai, I.; Brunvoll, J.; Kolonits, M.; Khodorkovsky, V. *J. Mol. Struct.* **1994**, *317*, 273.

(5) Blöchl, P. E. *Phys. Rev. B* **1994**, *50*, 17953.

(6) Car, R.; Parrinello, M. *Phys. Rev. Lett.* **1985**, *55*, 2471.

(7) Margl, P.; Schwarz, K.; Blöchl, P. E. *J. Chem. Phys.* **1994**, *100*, 8194.

(8) Perdew, J. P.; Zunger, A. *Phys. Rev. B* **1981**, *23*, 5048.

(9) Ceperley, M.; Adler, B. L. *Phys. Rev. Lett.* **1980**, *45*, 566.

(10) Becke, A. D. *J. Chem. Phys.* **1992**, *96*, 2155.

(11) Perdew, J. P. *Phys. Rev. B* **1986**, *33*, 8822.

(12) Blöchl, P. E. *J. Chem. Phys.* **1995**, *103*, 7422.

(13) Nosé, S. *J. Chem. Phys.* **1984**, *81*, 511, S. Nosé, *Mol. Phys.* **1984**, *52*, 255.

(14) Verlet, L. *Phys. Rev.* **1967**, *159*, 98.

(15) Kohanoff, J. *Comput. Mater. Sci.* **1994**, *2*, 221. Kohanoff, J.; Andreoni, W.; Parrinello, M. *Phys. Rev. B* **1992**, *46*, 4371.

(16) Becke, A. D. *J. Chem. Phys.* **1993**, *98*, 5648.

(17) Faulhaber, J. C. R.; Ko, D. Y. K.; Briddon, P. R. *Synth. Met.* **1993**, *60*, 227.

(18) Cooper, W. F.; Kenny, N. C.; Edmonds, J. W.; Nagel, A.; Wudl, F.; Coppens, P. *Chem. Commun.* **1971**, 889.

(19) Le Cointe, M.; Lemée-Cailleau, M. H.; Cailleau, H.; Toudic, B.; Toupet, L.; Heger, G.; Moussa, F.; Schweiss, P.; Kraft, K. H.; Karl, N. *Phys. Rev. B* **1995**, *51*, 3374.

(20) Clemente, D. A.; Marzotto, A. *J. Mater. Chem.* **1996**, *6*, 941.

(21) Umland, T. C.; Allie, S.; Kuhlmann, T.; Coppens, P. *J. Phys. Chem.* **1988**, *92*, 6456.

(22) Flandrois, S.; Chasseau, D. *Acta Crystallogr.* **1977**, *B33*, 2744.

(23) Guionneau, P.; Kepert, C. J.; Bravic, G.; Chasseau, D.; Truter, M. R.; Kurmoo, M.; Day, P. *Synth. Met.* **1997**, *86*, 1973.

(24) Lichtenberger, D. L.; Johnston, R. L.; Hinkelmann, K.; Suzuki, T.; Wudl, F. *J. Am. Chem. Soc.* **1990**, *112*, 3302.

(25) Haddon, R. C. *Aust. J. Chem.* **1975**, *28*, 2333.

(26) Katan, C.; Koenig, C. To be published.

(27) Murase, M.; Konno, M.; Matsuzaki, S.; Hiejima, T.; Sano, S. 59th National Meeting of the Chemical Society of Japan, Yokohama, March 1990; Abstr. 2F212.

(28) Katan, C.; Blöchl, P.; Margl, P.; Koenig, C. *Phys. Rev. B* **1996**, *53*, 12112.

(29) Fortunelli, A.; Painelli, A. *J. Chem. Phys.* **1997**, *106*, 8051.

(30) Carloni, P.; Blöchl, P. E.; Parrinello. M. *J. Phys. Chem.* **1995**, *99*, 1338.

(31) Castet, F.; Fritsch, A.; Ducasse, L. *J. Phys. I (Fr.)* **1996**, *6*, 583.

(32) Sato, N.; Inokuchi, H.; Shirotani, I. *Chem. Phys.* **1980**, *60*, 327.

(33) Batsanov, A. S.; Bryce, M. R.; Heaton, J. N.; Moore, A. J.; Skabara, P. J.; Howard, J. A. K.; Orti, E.; Viruela, P.; Viruela, R. *J. Mater. Chem.* **1995**, *5*, 1689.

(34) Pecile, C.; Painelli, A.; Girlando, A. *Mol. Cryst. Liq. Cryst.* **1989**, *171*, 69.

(35) Bozio, R.; Girlando, A. Pecile, D. *Chem. Phys. Lett.* **1977**, *52*, 503, Bozio, R.; Zanon, I.; Girlando, A.; Pecile, D. *J. Chem. Phys.* **1979**, *71*, 2282.

(36) Moreac, A.; Girard, A.; Delugeard, Y.; Marqueton, Y. *J. Phys.: Condensed Matter* **1996**, *8*, 3553.

(37) Moreac, A.; Girard, A.; Delugeard, Y. *J. Phys.: Condensed Matter* **1996**, *8*, 3569.

(38) Inoue, M. B.; Inoue, M.; Fernando, Q.; Nebesny, K. W. *Inorg. Chem.* **1986**, *25*, 3976.

(39) Girlando, A.; Marzola, F.; Pecile, C. *J. Chem. Phys.* **1983**, *79*, 1075.

(40) Berlinsky, A. J.; Hoyano, Y.; Weiler, L. *Chem. Phys. Lett.* **1977**, *45*, 419.